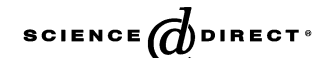


Available online at www.sciencedirect.com





Atmospheric Environment 40 (2006) 5508-5521

www.elsevier.com/locate/atmosenv

# Air quality impacts of distributed power generation in the South Coast Air Basin of California 1: Scenario development and modeling analysis

M.A. Rodriguez, M. Carreras-Sospedra, M. Medrano, J. Brouwer, G.S. Samuelsen, D. Dabdub\*

Department of Mechanical and Aerospace Engineering, Henry Samueli School of Engineering, 4200 Engineering Gateway Building, University of California, Irvine, CA 92697-3975, USA

Received 21 December 2004; received in revised form 5 July 2005; accepted 5 July 2005

#### Abstract

Distributed generation (DG) is generally defined as the operation of many small stationary power generators throughout an urban air basin. Although DG has the potential to supply a significant portion of the increased power demands in California and the rest of the United States, it may lead to increased levels of in-basin pollutants and adversely impact urban air quality. This study focuses on two main objectives: (1) the systematic characterization of DG installation in urban air basins, and (2) the simulation of potential air quality impacts using a state-of-the-art three-dimensional computational model. A general and systematic approach is devised to construct five realistic and 21 spanning scenarios of DG implementation in the South Coast Air Basin (SoCAB) of California. Realistic scenarios reflect an anticipated level of DG deployment in the SoCAB by the year 2010. Spanning scenarios are developed to determine the potential impacts of unexpected outcomes. Realistic implementations of DG in the SoCAB result in small differences in ozone and particulate matter concentrations in the basin compared to the baseline simulations. The baseline accounts for population increase, but does not consider any future emissions control measures. Model results for spanning implementations with extra high DG market penetration show that domain-wide ozone peak concentrations increase significantly. Also, air quality impacts of spanning implementations when DG operate during a 6-h period are larger than when the same amount of emissions are introduced during a 24-h period.

© 2006 Published by Elsevier Ltd.

Keywords: Distributed power generation; Air quality modeling; Ozone; PM2.5; South Coast Air Basin of California

#### 1. Introduction

Distributed generation (DG) has the potential to supply a significant portion of the increasing power

\*Corresponding author. Tel.: +19498246126; fax: +19498248585.

E-mail address: ddabdub@uci.edu (D. Dabdub).

demands in California and elsewhere (CEC, 1999). Recently, Gellins and Yeager (2004) considered that DG is one of the emerging technologies that will transform the electric infrastructure into a smart power system capable of supporting the needs of the digital society of the 21st century. DG entails the use of power generation technologies (e.g., fuel cells, gas turbines) to produce electricity and thermal

energy for local use. Emissions from DG units are characterized by many small point sources allocated throughout urban air basins. In contrast, centralgeneration sources are typically located outside air basins. DG technologies can fulfill the energy needs of numerous customers and provide overall emissions reduction, energy efficiency and cost savings in multiple applications. For instance, DG units can deliver critical customer loads with emergency stand-by power; support available capacity to meet peak power demands; improve user power quality; and provide low-cost total energy in combined cooling, heating and power (CHP) applications.

Recently, California is reorganizing its electric power industry. Today more than 2000 MW can be classified as DG according to the DG strategic plan developed by the California Energy Commission (Tomashefsky and Marks, 2002). Due to grid constraints, growing power demands and high cost power, California is one of the first places where DG adoption may become widespread. Distributed generation technology is currently approved for installation and regular use in the South Coast Air Basin (SoCAB) of California by two separate procedures, depending upon the size of the DG unit. Units smaller than 1 MW can be installed in the SoCAB after being certified by the California Air Resources Board as meeting the 2003 or 2007 standards for DG emissions. Larger DG units are permitted by the South Coast Air Quality Management District (SCAOMD) and are required to meet the Best Available Control Technology (BACT) emissions limits established by SCAOMD. Currently diesel generators cannot meet the emissions standards for continuous operation under either the CARB certification or SCAQMD permitting processes. Diesel generators can only meet emissions limits that are placed as back-up generators. Consequently, diesel engines are not considered in the current study. In other areas, emissions standards may be sufficiently less stringent that diesel generators may need to be considered in the mix of DG technologies.

The shift from central to distributed power generation may increase basin pollutant emissions and lead to higher levels of ambient ozone and particulate matter concentrations. Researchers have examined some air quality impacts due to DG emissions (Allison and Lents, 2002; Ianucci et al., 2000). However, these studies are limited to the evaluation of total emissions only. Furthermore, Heath et al. (2003) considered the potential for

increased human inhalation exposure to air pollutants when power plants are replaced by DG units. Yet, Heath et al. (2003) limited their work to pollutants emitted directly into the atmosphere using a simplified mass transport approach. Determination of potential air quality impacts of DG requires understanding of the spatial and temporal emission profiles and subsequent analysis of DG emissions impacts using a detailed atmospheric chemistry transport model.

The installation of DG units in urban air basins raises numerous concerns that must be addressed before any public policy decisions are made to allow, support or regulate DG implementation. Namely, how will DG likely be adopted in the South Coast Air Basin (SoCAB) of California? Will increased emissions from DG units affect the levels of ambient ozone with respect to the 8-h ozone standard? Could any increase in  $NO_x$  emissions enhance secondary particulate matter formation? What DG implementation scenarios could reduce overall environmental impacts?

The present study is the first to address these questions. This work characterizes the implementation of DG in the SoCAB with a comprehensive set of realistic scenarios developed with a general and systematic approach. Furthermore, the potential air quality impacts for each scenario are evaluated with numerical simulations performed in a detailed threedimensional air quality model (AQM). The methodology used in the development of DG implementation scenarios and the specific conditions to perform the simulations with the computational model are reported in Section 2. Results of a base case simulation used for comparison with DG implementation scenarios are presented in Section 3. Finally, in-depth analysis of the potential air quality impacts of DG implementation is presented in Section 4.

## 2. Scenario development

A comprehensive evaluation of potential DG air quality impacts requires a detailed description of a series of parameters that fully characterize a DG scenario. These parameters define the type and performance of DG units, the spatial and temporal distribution of DG operation throughout the basin, and other features related to the particular use of DG. This section presents a general and systematic approach to develop several scenarios of DG adoption. Each scenario is then associated to a

corresponding emissions inventory. Finally, the assessment of DG air quality impacts relies on these emission inventories as input for the computational air quality model.

In this work, a DG scenario is described completely when the following seven parameters are fully determined (Medrano et al., 2003): the fraction of energy needs met by DG; the DG mix of technologies; the emissions profile of each DG technology; the spatial distribution of DG deployment in the SoCAB; the DG duty cycle; the emissions displaced; and other estimates such as DG degradation rates, emissions speciation and the curve of cumulative DG power use, i.e., the total cumulative DG power implemented in the basin over time. Once a DG scenario is constructed, the corresponding emissions are determined for each cell in the computational domain.

The development of scenarios from all possible combinations and permutations of DG deployment parameters is infeasible and inefficient. Therefore, DG scenarios are classified into two major categories: realistic and spanning scenarios. Realistic scenarios reflect an anticipated level of DG deployment in the SoCAB by the year 2010 and include the use of DG market penetration studies; end user specific energy demand profiles and technology preferences; and relies on spatially resolved geographic information systems (GIS) data. In contrast, spanning scenarios are developed for scientific completeness and determination of potential impacts from unexpected outcomes. A total of five realistic and 21 spanning scenarios are developed using these two major categories. Table 1 presents a detailed summary of all spanning and realistic scenarios formulated. The following sections detail the specific methodologies used to devise all scenarios. In most cases, DG implementation results in increase of primary pollutants emissions. Some scenarios, however, account for emissions displacement that leads to an overall decrease in emissions of certain pollutants.

Emissions displacement by DG occurs in various ways, only three of which are noted herein. First, DG can replace older energy conversion equipment of lower efficiency and higher emissions, leading to a net reduction in emissions of both CO<sub>2</sub> and other pollutants. Second, DG units will typically produce a waste heat stream in addition to electricity. If this waste heat stream is used for industrial process heating instead of using boilers or water heaters, then the emissions previously associated with these

boilers are displaced. Third, DG could be used in new applications where they would emit less pollutants than the current means to meet a power demand. An example is the elimination of the idling of ships while in port by producing sufficient electricity in the port to meet the power requirements of docked ships. This would displace a fraction of the previous ship emissions through use of more efficient and clean DG devices.

#### 2.1. Realistic scenarios

Samuelsen et al. (2003) formulated a 10-step methodology to construct realistic scenarios with a general and systematic strategy. This methodology incorporates high-resolution geographic information systems (GIS) land-use data, available for more than 132 land-use types with an area resolution of two-acres (P. Gutierrez, Southern California Association of Governments, personal communication, 2002). Fig. 1 summarizes the methodology used to characterize a DG realistic scenario. The formulation starts by defining six market sectors that aggregate the original 13 high-level GIS land-use types. Market sectors are categories such as residential, commercial, industrial, and institutional sectors, in which the market is divided based on the type of economic activity. Each market sector is subdivided into six size categories according to power demand and the corresponding DG power capacity (<50, 50-250, 250-1000 kW, 1-5, 5-20, and 20-50 MW). Thus, each computational cell contains different land areas associated to the combination of six market sectors and six size categories per sector. DG power is determined using the relative intensity adoption rate: a factor that relates the land-use area to the relative amount of DG power adopted as a function of size category and market sector. Intensity factors are based on reported CHP penetration in the commercial and industrial sectors in California (CEC, 1999). The temporal variation of DG power is determined using average load profiles for each sector that the DG units serve. Average load profiles are calculated for each market sector based on hourly sector electric demand data from Southern California Edison (SCE, 2002). For each market sector, the relative contributions to total power by every DG type and size category are considered. DG types include high and low temperature fuel cells (FC); micro-turbine generators (MTGs); natural gas internal combustion engines (NG-ICEs);

Table 1 Summary of realistic and spanning scenarios

Name	Common parameters	Increased power demand %	DG power adoption	CHP displacement
R1	Technology mix depends on activity	5	Linear	Yes
R2	sector, high penetration of low	10	Linear	Yes
R3	emission technologies, GIS land use	20	Linear	Yes
R4	distribution, realistic duty cycles, and	5	Low early <sup>a</sup>	Yes
R5	low performance degradation	5	Linear	No

#### Spanning scenarios

Name	Short description	Increased power demand %	Spatial distribution	Technology mix <sup>b</sup> %				
				GT	NG-ICE	MTG	FC	PV
PW2010	Population weighted 2010	20	PW <sup>c</sup>	30	30	25	7	8
2003ES	2003 emission standards	20	PW	_	-	_	_	_
2007ES	2007 emission standards	20	PW	_	_	_	_	_
PermICEPW20	Permitted NG-ICE	20	PW		100			
HEAPW20	High early adoption of DG	20	PW	30	30	25	7	8
PeakPW	Peaking duty cycle	20	PW	35	35	30		
LDG20	Large DG (GT)	20	$HIA^d$	100				
NH3_20	Ammonia from GT considered	20	HIA	100				
PGW20	Population growth-weighted	20	$PGW^{e}$	30	30	25	7	8
LUW20	Land-use weighted	20	$LUW^f$	30	30	25	7	8
Free20	Freeways density-weighted	20	FreeW <sup>g</sup>	30	30	25	7	8
FCPW20	All DG are FC	20	PW				100	
MTGPW20	All DG are MTG	20	PW			100		
DGCHP	CHP emissions displaced	20	PW	30	30	25	7	8
DGEED	Electricity emissions displaced	20	PW	35	35	30		
TDPW10	Technology distribution	10	PW		34	46	10	10
BAU	Business as usual	Linear	PW	52	28	4	1	15
EHP	Extra high penetration	20 total <sup>h</sup>	PW	30	30	25	7	8
BAU_par	Business as usual (parabolic)	Quadratic	PW	52	28	4	1	15
HPD_	High performance degradation	20	PW	30	30	25	7	8
PeakPW_2	Peaking duty cycle	80	PW	35	35	30		

<sup>&</sup>lt;sup>a</sup>98% of DG installed between 2007 and 2010.

photovoltaics (PV); gas turbines (GT); Stirling engines, and hybrid fuel cell gas turbine systems. Weighting factors are applied to account for the relative DG adoption rates that vary with location inside the basin. The DG scenarios developed in this effort are not based upon a detailed market penetration analysis for each DG technology type in the SoCAB, but rather upon currently available studies in the literature, authors insights, and DG

stakeholder feedback. Resources used include: previous studies that determined a reasonable mix of technologies (Ianucci et al., 2000; Marnay et al., 2001); input from industry stakeholder workshops; authors current understanding of technology features; current penetration of certain technologies (e.g., MTGs); and authors intuition, engineering insight and/or brainstorming. From these estimates the "DG adoption factor" was established as a

<sup>&</sup>lt;sup>b</sup>Gas turbines (GT), Natural gas internal combustion engines (NG-ICE), Micro-turbine generators (MTG), Fuel cells (FC), Photovoltaics (PV).

<sup>&</sup>lt;sup>c</sup>PW: Population-weighted.

<sup>&</sup>lt;sup>d</sup>HIA: Highly industrialized areas.

<sup>&</sup>lt;sup>e</sup>PGW: Population growth-weighted.

<sup>&</sup>lt;sup>f</sup>LUW: Land-use-weighted.

<sup>&</sup>lt;sup>g</sup>FreeW: Freeways density-weighted.

<sup>&</sup>lt;sup>h</sup>20% of total power met by DG.

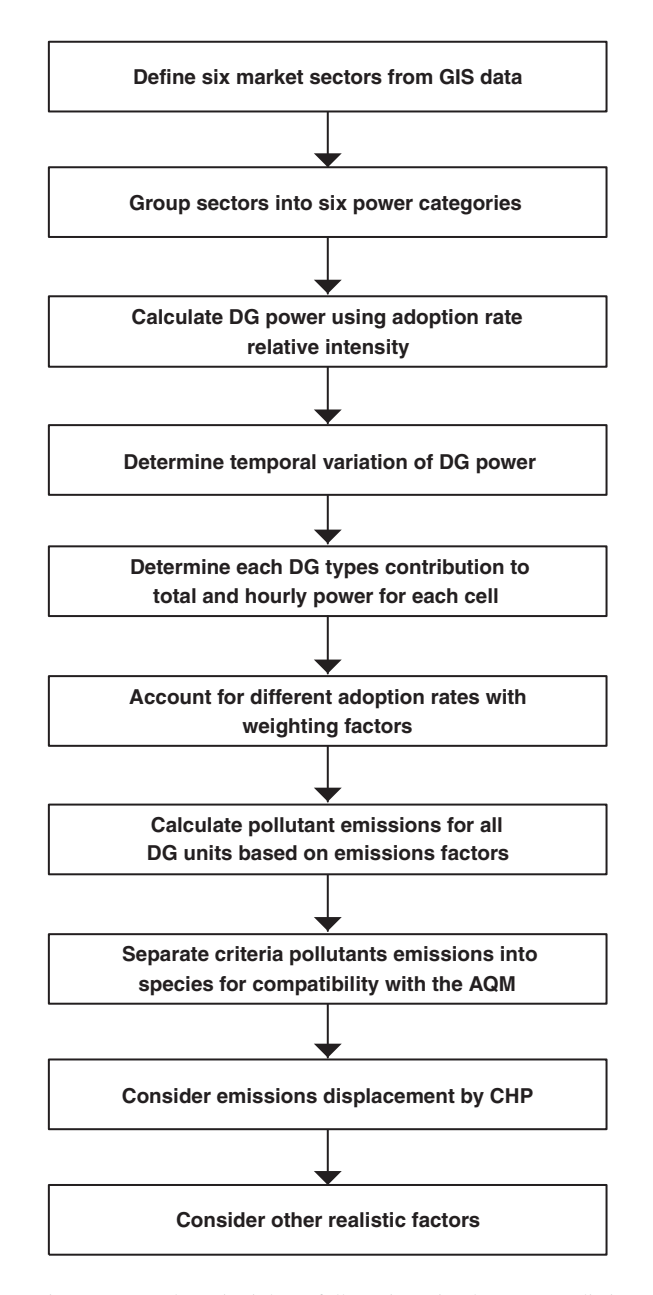


Fig. 1. General methodology followed to develop DG realistic scenarios.

relative market penetration weighting of each of the DG types in each of the market sectors considered. Using the GIS data for spatial location of various market sectors together with these market penetration estimates, a particular weighting factor for each type of DG technology and its relative magnitude of market adoption was derived and applied in each of the model cells.

For each DG type, hourly pollutant emissions estimated for every cell are based on emission factors from reported estimates (Allison and Lents, 2002; Ianucci et al., 2000; Marnay et al., 2001) and measurements (Phi et al., 2004). In all cases, DG emissions within the SoCAB never exceed the applicable South Coast Air Quality Management District (SCAQMD) and California Air Resources Board (CARB) emission limits. Current CARB emmision standards for DG units installed before 2007 are less stringent than those installed on or after January 1, 2007. Tables 2 and 3 show the emissions factors used to develop DG Scenarios in the current study for DG units installed in the periods 2003–2006 and 2007–2010, respectively. The units in the table represent lbs of each pollutant emissions considered per unit of energy (kWh) produced by the particular DG unit type.

Generally, air quality models require further speciation of emissions for most pollutants ( $NO_x$ , VOC,  $SO_x$ , and PM). Thus specific mass fluxes of NO, NO<sub>2</sub>, SO<sub>2</sub>, SO<sub>3</sub>, 23 specific volatile organic compounds, 18 types and eight size classes of particulate matter are considered according to the Caltech Atmospheric Chemistry Mechanism (CACM) (Griffin et al., 2002a, 2002b; Pun et al., 2002). Emissions displacement is accounted for when DG installations include CHP. Several parameters for emissions displacement are estimated such as the fraction of DG installed technologies that include CHP; the average heat recovery capacity factor; the old and new boiler mix being displaced, and their corresponding efficiencies and emission factors. Finally, other factors that can affect the final emissions levels are included for the particular year of interest. These factors include the rates at which individual DG technologies will be adopted versus time, and performance degradation of the particular DG units from the date they are installed until the target year of simulation.

In general, realistic DG implementation scenarios introduce mass increments no larger than 0.43% with respect to baseline emissions. The distribution of these sources concentrates DG technologies with high emission factors nearby industrial zones such as Long Beach and Los Angeles where the market research, power and energy demands favor more DG use. In contrast, the population-weighted distribution of DG, used in most of the spanning scenarios, is relatively smooth throughout the domain and places DG predominantly in the central area of Los Angeles. Realistic scenario R1 serves as

Table 2
Emissions factors used to develop DG scenarios in the current study for DG units installed in the period 2003–2006

Generation type	Efficiency <sup>a</sup>	CO (lbs kWh <sup>-1</sup> )	VOC	$NO_x$	$SO_x$	PM	CO <sub>2</sub>	NH <sub>3</sub>
MTG <sup>b</sup>	0.270	$2.85 \times 10^{-3}$	$5.00 \times 10^{-5}$	$7.00 \times 10^{-4}$	$1.01 \times 10^{-5}$	$8.35 \times 10^{-5}$	1.50	0
$GT(<3 \text{ MW})^c$	0.244	$3.12 \times 10^{-4}$	$3.58 \times 10^{-5}$	$4.62 \times 10^{-4}$	$1.12 \times 10^{-5}$	$9.23 \times 10^{-5}$	1.66	$1.70 \times 10^{-4}$
$GT(>3 \text{ MW})^d$	0.360	$2.12 \times 10^{-4}$	$2.43 \times 10^{-5}$	$1.26 \times 10^{-4}$	$7.59 \times 10^{-6}$	$6.26 \times 10^{-5}$	1.13	$6.42 \times 10^{-5}$
NG-ICE <sup>e</sup>	0.320	$1.77 \times 10^{-3}$	$4.43 \times 10^{-4}$	$4.43 \times 10^{-4}$	$8.54 \times 10^{-6}$	$7.04 \times 10^{-5}$	1.27	0
LT FC <sup>f</sup>	0.360	$1.00 \times 10^{-4}$	$9.00 \times 10^{-4}$	$7.00 \times 10^{-5}$	$7.59 \times 10^{-6}$	$6.26 \times 10^{-5}$	1.13	0
HT FC <sup>g</sup>	0.480	$1.00 \times 10^{-4}$	$2.00 \times 10^{-5}$	$7.00 \times 10^{-5}$	$5.69 \times 10^{-6}$	$4.69 \times 10^{-5}$	0.85	0
Stirling <sup>h</sup>	0.270	$6.00 \times 10^{-3}$	$1.00 \times 10^{-3}$	$5.00 \times 10^{-4}$	$1.01 \times 10^{-5}$	$8.35 \times 10^{-5}$	1.50	0
Hybrid <sup>i</sup>	0.700	$6.00 \times 10^{-3}$	$1.00\times10^{-3}$	$5.00 \times 10^{-4}$	$3.90\times10^{-6}$	$3.22\times10^{-5}$	0.58	0

<sup>&</sup>lt;sup>a</sup>Net efficiency of the device on the basis of the higher heating value (HHV) of the fuel used. This is equal to the net electrical energy produced by the unit divided by the HHV of the fuel.

Table 3
Emissions factors used to develop DG scenarios in the current study for DG units installed in the period 2007–2010

Generation type	Efficiency <sup>a</sup>	CO (lbs kWh <sup>-1</sup> )	VOC	$NO_x$	$SO_x$	PM	CO <sub>2</sub>	NH <sub>3</sub>
MTG <sup>b</sup>	0.270	$1.00 \times 10^{-4}$	$2.00 \times 10^{-5}$	$7.00 \times 10^{-5}$	$1.01 \times 10^{-5}$	$8.35 \times 10^{-5}$	1.50	0
$GT(<3 \text{ MW})^c$	0.244	$3.12 \times 10^{-4}$	$3.58 \times 10^{-5}$	$4.62 \times 10^{-4}$	$1.12 \times 10^{-5}$	$9.23 \times 10^{-5}$	1.66	$1.70 \times 10^{-4}$
$GT(>3 \text{ MW})^d$	0.360	$2.12 \times 10^{-4}$	$2.43 \times 10^{-5}$	$1.26 \times 10^{-4}$	$7.59 \times 10^{-6}$	$6.26 \times 10^{-5}$	1.13	$6.42 \times 10^{-5}$
NG-ICE <sup>e</sup>	0.320	$1.77 \times 10^{-3}$	$4.43 \times 10^{-4}$	$4.43 \times 10^{-4}$	$8.54 \times 10^{-6}$	$7.04 \times 10^{-5}$	1.16	0
LT FC <sup>f</sup>	0.360	$1.00 \times 10^{-4}$	$2.00 \times 10^{-5}$	$7.00 \times 10^{-5}$	$7.59 \times 10^{-6}$	$6.26 \times 10^{-5}$	1.13	0
HT FC <sup>g</sup>	0.480	$1.00 \times 10^{-4}$	$2.00 \times 10^{-5}$	$7.00 \times 10^{-5}$	$5.69 \times 10^{-6}$	$4.69 \times 10^{-5}$	0.85	0
Stirling <sup>h</sup>	0.270	$1.00 \times 10^{-4}$	$2.00 \times 10^{-5}$	$7.00 \times 10^{-5}$	$1.01 \times 10^{-5}$	$8.35 \times 10^{-5}$	1.50	0
Hybrid <sup>i</sup>	0.700	$1.00\times10^{-4}$	$2.00\times10^{-5}$	$7.00\times10^{-5}$	$3.90\times10^{-6}$	$3.22\times10^{-5}$	0.58	0

<sup>&</sup>lt;sup>a</sup>Net efficiency of the device on the basis of the higher heating value (HHV) of the fuel used. This is equal to the net electrical energy produced by the unit divided by the HHV of the fuel.

the reference for other realistic cases. Namely, the other four scenarios consider single variations of the parameters that define R1. R1 assumes that 5% of the increased power demand from 2002 to 2010 will be met by DG. The spatial distribution of DG is

based on land-use data and DG operation follows realistic duty cycles corresponding to different activity sectors in each computational cell. In addition, different DG technologies are deployed depending on the activity area of use. All the other

<sup>&</sup>lt;sup>b</sup>Micro-turbine generators.

<sup>&</sup>lt;sup>c</sup>Gas turbines with generation capacity up to 3 MW.

<sup>&</sup>lt;sup>d</sup>Gas turbines with generation capacity larger than 3 MW.

<sup>&</sup>lt;sup>e</sup>Natural gas internal combustion engines.

<sup>&</sup>lt;sup>f</sup>Low temperature fuel cells.

gHigh temperature fuel cells.

<sup>&</sup>lt;sup>h</sup>Stirling engines.

<sup>&</sup>lt;sup>i</sup>Hybrid fuel cell gas turbine systems.

<sup>&</sup>lt;sup>b</sup>Micro-turbine generators.

<sup>&</sup>lt;sup>c</sup>Gas turbines with generation capacity up to 3 MW.

<sup>&</sup>lt;sup>d</sup>Gas turbines with generation capacity larger than 3 MW.

<sup>&</sup>lt;sup>e</sup>Natural gas internal combustion engines.

<sup>&</sup>lt;sup>f</sup>Low temperature fuel cells.

gHigh temperature fuel cells.

<sup>&</sup>lt;sup>h</sup>Stirling engines.

<sup>&</sup>lt;sup>i</sup>Hybrid fuel cell gas turbine systems.

realistic scenarios exhibit the same spatial and temporal emissions distribution as R1. Scenarios R2 and R3, however, implement a larger DG penetration, i.e., 10% and 20% of the increased power demand between 2002 and 2010, respectively. Emission displacement due to CHP applications is increased by the same proportion in R2 and R3 with respect to R1. The DG adoption rate in scenario R4 assumes an exponential DG adoption rate leading to 98% of the DG technologies being installed after the year 2007. R4 is also the scenario with the lowest CO and VOC emissions. Finally, scenario R5 neglects emissions displacement due to CHP and has the highest NO<sub>x</sub> emissions.

## 2.2. Spanning scenarios

Spanning scenarios provide insights on the relative impacts of several parameters, such as the extent of DG market penetration, the DG mix of technologies, the emissions displacement, the DG spatial distribution, and the DG duty cycles. In most cases, a total DG power penetration is assumed and allocated among computational cells in the SoCAB proportional to either population or population growth. Next, a pre-determined mix of DG technologies is applied to all cells and pollutant emissions estimated from the mix.

Most spanning scenarios consider the spatial distribution of DG throughout the SoCAB proportional to population density. However, another set of scenarios is developed to determine the effects of other spatial distributions. For instance, PGW20 assumes a DG distribution proportional to population growth from 2000 to 2010, whereas Free20 is proportional to the freeway density. Most spanning scenarios assume that 20% of the increased power demand from 2002 to 2010 will be met by DG. Also, with the exception of three scenarios accounting for duty cycles, it is assumed that DG units operate continuously throughout the day. Finally, different sets of DG technology types are considered, including scenarios in which fuel cells, MTG, gas turbines or NG-ICE are permitted to operate exclusively.

#### 2.3. Simulation conditions

Once the emission inventories are estimated for each scenario, numerical simulations are performed using the California Institute of Technology (CIT) air quality model. The CIT Airshed model has been

used extensively to investigate the formation of ozone and particulate matter in the SoCAB (Meng et al., 1998; Nguyen and Dabdub, 2002b; Griffin et al., 2002b, 2004). The CIT Airshed model is a threedimensional Eulerian photochemical model that predicts air pollutant concentrations undergoing chemical reactions, deposition and transport. The computational domain includes a large part of the SoCAB with a horizontal resolution of 5 by 5 km. Vertically, five non-uniform layers span up to 1100 m above the surface of the SoCAB terrain. The model includes a comprehensive size- and chemically resolved aerosol module (Meng et al., 1998; Griffin et al., 2002a, 2002b). Statistical analyses by Griffin et al. (2002a) show there is a good correlation between simulation results and measured data. Scenarios are simulated under the same meteorological conditions of the Southern California Air Quality Study (SCAQS) episode on August 27-29th, 1987. These conditions enhance smog formation and are typical of non-attainment days in the SoCAB. To minimize the influence of initial conditions a three-day episode is run with the CIT model for all scenarios. Results reported in this study correspond to the third day of simulations.

## 3. Baseline scenario

Prior to establishing any potential impacts of DG implementation in the SoCAB, a complete characterization of baseline results is necessary. SCAQMD and CARB have prepared emissions inventories to evaluate the control measures that lead to attainment of ozone federal air quality standards by the year 2010. These agencies have prepared two different emission inventories: baseline and attainment emissions inventories.

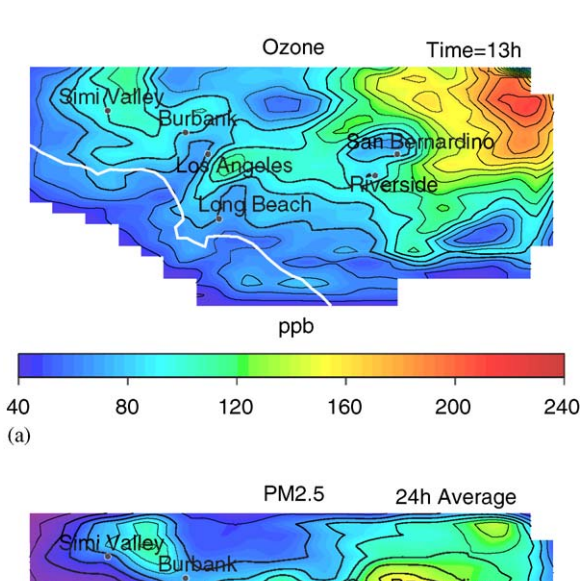
The baseline scenario accounts for population increase and power and transportation demands increases, but does not consider any future emissions control measures or contributions due to DG power. The attainment scenario, on the other hand, includes all the control measures proposed by the state agencies to accomplish the federal air quality standards for ozone by the year 2010. The present study uses the baseline emissions inventory since the attainment emissions inventory remains under revision and development. DG air quality impacts, however, may be significantly higher if the attainment scenario were to have been used instead. For instance, VOC and NO<sub>x</sub> emissions in the attainment

inventory are lower than those in the baseline by 50% and 32%, respectively.

Table 4 summarizes the values for the maximum concentration of some criteria pollutants using the 2010 baseline emission inventory. Fig. 2 shows that secondary pollutants (ozone, NO<sub>2</sub> and PM<sub>2.5</sub>) peak downwind from high-emissions locations (Central

Table 4 Simulated concentrations of some criteria pollutants using the 2010 baseline scenario. Maximum hourly average concentration for O<sub>3</sub>, NO<sub>2</sub>, and CO. 24-h average concentration for PM<sub>2.5</sub>

Species	Maximum	Location	Average	Time
O <sub>3</sub> NO <sub>2</sub> CO PM <sub>2.5</sub>	238 ppb 158 ppb 3 ppm 115 μg m <sup>-3</sup>	San Bernardino Ontario Los Angeles Riverside	1-h average 1-h average 1-h average 24-h average	13:00 5:00 8:00



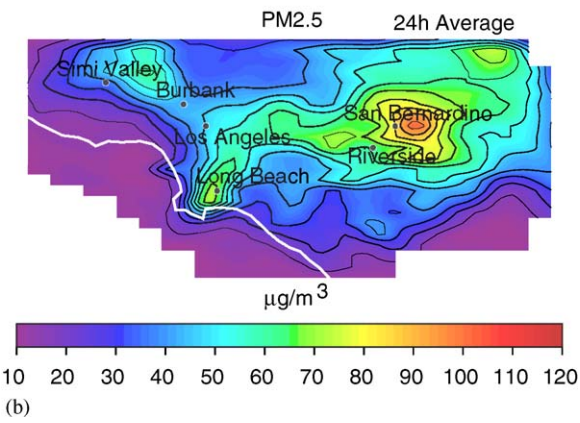


Fig. 2. Criteria pollutants concentrations for 2010 baseline simulation: (a) Ozone at hour 13:00, (b) 24-h average  $PM_{2.5}$  concentration.

Los Angeles), whereas CO peaks in Los Angeles because its concentration depends on direct emissions. Ozone and PM<sub>2.5</sub> modeled concentrations exceed current federal air quality standards since the emissions inventory used does not include prospective air pollution control measures to be implemented before 2010. Furthermore, it accounts for population growth with the corresponding increase in anthropogenic emissions.

## 4. Air quality impacts of DG scenarios

The following sections present a summary of the observed effects on air quality for all realistic and some selected spanning scenarios. A thorough description and analysis of the complete set of 26 DG scenarios developed is found in Samuelsen et al. (2004).

#### 4.1. Realistic scenarios

Table 5 compares the basin-wide impacts on  $O_3$ ,  $NO_2$  and  $PM_{2.5}$  concentrations for all realistic

Table 5 Maximum ozone,  $NO_2$  and 24-h average  $PM_{2.5}$  concentrations for realistic scenarios. Also shown is the largest difference (maximum and minimum) with respect to the baseline scenario. Baseline columns show the hourly concentration reference values that correspond (in time and space) to the maximum or minimum difference on the right. Except for  $PM_{2.5}$ , values are reported at specific hours shown in parentheses

Scenario	Max	Baseline	$Max(\Delta^a)$	Baseline	Min(△)
O <sub>3</sub> (ppb)					
R1	238(13:00)	46(13:00)	3	60(12:00)	-2
R2	238(13:00)	45(14:00)	5	152(13:00)	<b>-9</b>
R3	238(13:00)	89(12:00)	5	178(13:00)	-4
R4	238(13:00)	70(11:00)	3	178(13:00)	-8
R5	238(13:00)	88(12:00)	2	178(13:00)	-8
NO <sub>2</sub> (ppb	)				
R1	158(5:00)	93(1:00)	2	60(1:00)	-1
R2	158(5:00)	83(1:00)	2	57(18:00)	-3
R3	158(5:00)	83(1:00)	2	49(21:00)	-3
R4	158(5:00)	49(6:00)	3	6(18:00)	-3
R5	158(5:00)	18(23:00)	1	60(1:00)	-1
PM <sub>2.5</sub> (μg	$m^{-3}$ )				
R1	115	45	3	44	-2
R2	115	58	2	81	-2
R3	115	39	2	70	-2
R4	115	39	2	69	-2
R5	115	39	3	115	-3

 $<sup>^{</sup>a}\Delta = Realistic - Baseline.$ 

scenarios. Domain-wide maximum ozone and  $NO_2$  concentrations are constant among simulated scenarios. However, the largest hourly changes in  $NO_2$  range from -3 to 3 ppb. The domain-wide hourly maximum  $PM_{2.5}$  concentrations in all realistic scenarios are equal to the baseline peak. Hourly concentrations show more variation. Namely,  $PM_{2.5}$  decreases  $33 \, \mu g \, m^{-3}$  in R1 and increases  $17 \, \mu g \, m^{-3}$  in R5 with respect to the baseline. On the other hand, changes in 24-h average  $PM_{2.5}$  concentration fall within the range of  $\pm 3 \, \mu g \, m^{-3}$ .

Ozone concentrations differences between baseline and realistic scenarios range from -9 to 5 ppb. For R1, the maximum difference in ozone concentrations is on the order of 3 ppb. This occurs in areas where ozone concentrations are already low and more importantly in compliance with air quality standards. Fig. 3 shows the ozone difference between R1 and the baseline scenarios at peak concentrations (13:00). The most significant ozone

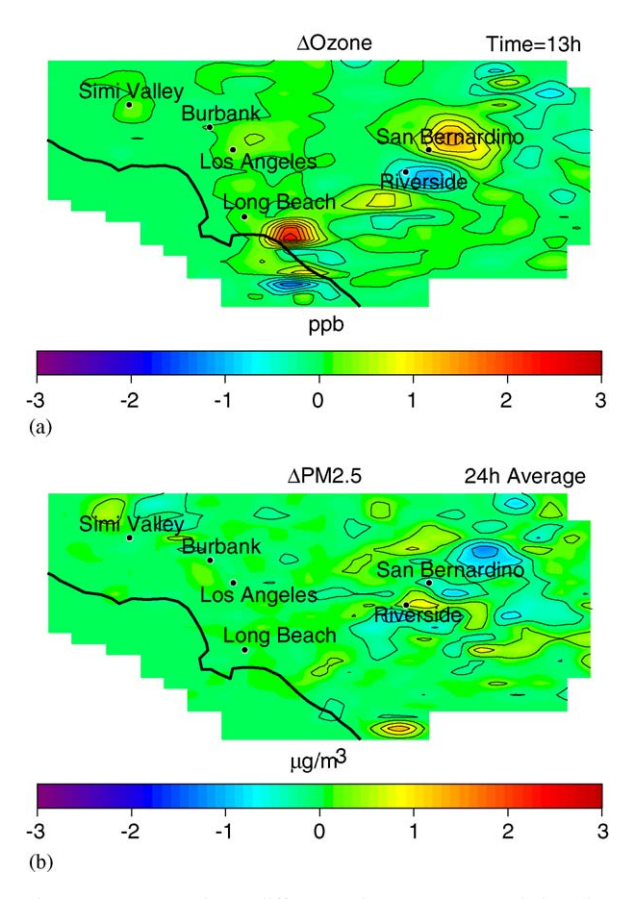


Fig. 3. Concentrations difference between R1 and baseline scenarios. (a) Ozone difference shown at hour 13:00. (b)  $PM_{2.5}$  difference shown for 24-h average concentrations.

decrease is less than 2 ppb and overall ozone concentrations are not affected by the increase in emissions due to scenario R1. Impacts on NO2 range between -1 and 2 ppb. The largest impacts occur at night and early morning, when NO2 is not photolyzed yet and concentrations are typically high. At night, NO<sub>2</sub> reacts with the remaining ozone to form NO<sub>3</sub>, the predominant atmospheric oxidant for unsaturated hydrocarbons and a precursor of particular matter. Thus, the maximum increase in particulate matter occurs during the early morning after NO2 peaks. Although model results show changes in hourly PM<sub>2.5</sub> concentrations, there are no significant impacts on PM<sub>2.5</sub> 24-h average concentrations (Fig. 3). Differences between R1 and the baseline for PM<sub>2.5</sub> 24-h average concentrations (-2 to  $3 \mu g m^{-3}$ ) occur near San Bernardino and Riverside, where typically maximum concentrations of particulate matter are observed. Air quality impacts are analyzed where anthropogenic emissions are high in the SoCAB (Los Angeles) and downwind from this region (Riverside). For scenario R1, ozone concentrations are nearly identical to the baseline at both locations. Also, impacts on PM<sub>2.5</sub> concentrations are marginal. However, they are more noticeable in Riverside than Central Los Angeles. Larger variability at Riverside is expected since PM<sub>2.5</sub> formation in this region is subjected to the availability of local ammonia emissions and nitric acid transported from central areas of the basin. Differences between base case and DG scenarios for PM<sub>2.5</sub> reach values up to  $\pm 5 \,\mu \mathrm{g \, m^{-3}}$ in Riverside.

The effects on pollutants as DG market penetration increases are also investigated. In scenarios R1, R2 and R3 ozone concentrations maximum difference with respect to baseline values range from -9to  $5 \,\mu g \, m^{-3}$ . However, in R2 and R3 the area where ozone concentrations are impacted increases due to progressively higher DG penetration. All five realistic scenarios show similar impacts on PM<sub>2.5</sub> concentrations. Nonetheless, the effects on PM<sub>2.5</sub> produced by increasing DG penetration are less evident than that of ozone. A scenario in which NO<sub>x</sub> emissions increase is R5 because it does not consider emissions displacement. The increase occurs mainly in the basin's central area and leads to slight reductions in ozone concentrations at hour 13:00. The decrease in ozone is expected given the high NO<sub>x</sub>/VOC ratio, characteristic of the Los Angeles area. Although ozone reductions are achieved in scenario R5 due to increased NO<sub>x</sub> emissions, they occur in locations where compliance with ozone air quality standards is already attained.

## 4.2. Spanning scenarios

The following section describes relevant results for simulations performed with spanning scenarios. A general overview is presented here. However, a complete report of modeling results for each spanning scenario is described by Samuelsen et al. (2004). Additionally, spanning scenarios are compared within different sub-categories that allow a parametric evaluation of their air quality impacts. Two sub-categories are chosen to examine systematically the effect of changing some of the parameters that describe a DG scenario.

For each spanning scenario Tables 6 and 7 show the domain-wide maximum concentration and maximum changes with respect to baseline results of key species. Maximum ozone concentrations in scenarios 2003ES, HEAPW20, BAU\_par, PeakPW\_2 and EHP increase by 1 ppb, whereas in LDG20 decrease by 1 ppb. For all other spanning scenarios maximum ozone concentrations remain

unchanged. Differences with respect to baseline ozone concentrations generally vary from -8 to 8 ppb. About half of the scenarios show that maximum increase at ozone concentrations occur in locations where baseline ozone is already below the California Ambient Air Quality Standard (CAAQS, 90 ppb). The remaining scenarios exhibit the largest increase in places where baseline concentrations already exceed the CAAOS. Furthermore, scenarios LUW20, DGCHP, and BAU, show increases in areas where baseline ozone exceeds the National Ambient Air Quality Standard (120 ppb). The largest ozone reductions occur in places and hours where baseline concentrations are already lower than AQ standards. Maximum NO2 concentrations remain unchanged in all spanning scenarios except for scenario PeakPW 2, in which NO<sub>2</sub> increases by 1 ppb. For most scenarios, maximum hourly changes in NO2 concentrations fall within the range of  $\pm 10 \,\mathrm{ppb}$ . Only scenarios PeakPW and PeakPW\_2 produce higher increases (up to 14 ppb and 30 ppb, respectively). Scenario DGEED, in which DG displaces in-basin power plants, produces higher decreases (-39 ppb).

Table 6
Maximum ozone concentrations for spanning scenarios. Also shown is the largest difference (maximum and minimum) with respect to the baseline scenario. Baseline columns show the hourly concentration reference values that correspond (in time and space) to the maximum or minimum difference on the right. Values are reported at specific hours shown in parentheses

Scenario	Max	Baseline	$Max(\Delta^a)$	Baseline	$Min(\Delta)$
O <sub>3</sub> (ppb)					
PW2010	238(13:00)	46(13:00)	4	5(5:00)	-3
2003ES	239(13:00)	100(13:00)	6	12(6:00)	-4
2007ES	238(13:00)	100(13:00)	5	66(11:00)	-7
PermICEPW20	238(13:00)	100(13:00)	7	12(6:00)	-3
HEAPW20	239(13:00)	100(13:00)	6	5(5:00)	-3
PeakPW	238(13:00)	100(13:00)	5	24(5:00)	-13
LDG20	237(13:00)	46(11:00)	8	66(11:00)	-7
NH3 20	238(13:00)	73(12:00)	3	66(11:00)	-7
PGW20	238(13:00)	108(14:00)	6	5(5:00)	-2
LUW20	238(13:00)	134(13:00)	5	5(5:00)	-3
Free20	238(13:00)	89(12:00)	6	54(22:00)	-3
FCPW20	238(13:00)	53(12:00)	3	146(12:00)	-1
MTGPW20	238(13:00)	89(12:00)	5	90(13:00)	-2
DGCHP	238(13:00)	134(13:00)	4	60(12:00)	-2
DGEED	238(13:00)	7(22:00)	34	73(14:00)	-14
TDPW10	238(13:00)	89(12:00)	5	60(12:00)	-2
BAU	238(13:00)	134(13:00)	4	146(12:00)	-4
EHP	239(13:00)	46(14:00)	8	15(6:00)	-8
BAU_par	239(13:00)	108(14:00)	6	66(11:00)	-7
HPD	238(13:00)	100(13:00)	6	5(5:00)	-3
PeakPW_2	239(13:00)	10(2:00)	8	29(2:00)	-26

 $<sup>^{</sup>a}\Delta = Spanning - Baseline.$ 

Table 7 Maximum 24-h average  $PM_{2.5}$  concentrations for spanning scenarios. Also shown is the largest difference (maximum and minimum) with respect to the baseline scenario. Baseline columns show the concentration reference values that correspond (in time and space) to the maximum or minimum difference on the right

Scenario	Max	Baseline	Max(Δ <sup>a</sup> )	Baseline	Min(\(\Delta\))
$PM_{2.5}(\mu g  m^{-3})$					
PW2010	114	78	3	90	-1
2003ES	113	45	3	67	-2
2007ES	114	45	3	81	-4
PermICEPW20	114	82	2	69	-2
HEAPW20	117	39	3	69	-2
PeakPW	114	45	3	83	-2
LDG20	115	39	3	94	-2
NH3_20	113	39	2	82	-2
PGW20	115	39	3	62	-1
LUW20	115	45	3	17	-2
Free20	114	39	3	55	-2
FCPW20	115	64	2	87	-2
MTGPW20	114	59	3	104	-2
DGCHP	114	39	3	79	-2
DGEED	113	59	2	81	-4
TDPW10	114	39	3	46	-2
BAU	115	45	3	104	-2
EHP	115	45	4	17	-2
BAU_par	115	78	2	17	-2
HPD	114	39	2	69	-2
PeakPW_2	116	75	6	14	-2

 $<sup>^{</sup>a}\Delta = Spanning - Baseline.$ 

One-hour average maximum  $PM_{2.5}$  concentrations range from -1 to  $1 \, \mu g \, m^{-3}$ , whereas the largest hourly changes are approximately  $\pm 27 \, \mu g \, m^{-3}$ . In contrast, maximum changes in 24-h average  $PM_{2.5}$  vary from -4 to  $6 \, \mu g \, m^{-3}$  for all the scenarios.

## 4.2.1. Duty cycle

This section examines cases in which DG supplies most of its load capacity during specific times. NO<sub>x</sub> emissions in the SoCAB peak at rush hours during the morning and evening, whereas VOC emissions are usually related to industrial activity. NO<sub>x</sub> and VOC emissions are high during the day and decrease considerably at night. Scenarios PeakPW and PeakPW\_2 assume DG units operate for 6h throughout the day (12:00 to 18:00). Hence DG systems work mainly when baseline emissions are peaking. PeakPW considers that all DG installations have the capacity to supply 20% of the increased power demand from 2002 to 2010 during the peak hours of operation. PeakPW\_2 assumes the same daily energy supply as PW2010, but

delivered in only 6h of operation. DG power capacity supplied by DG in PeakPW\_2 is then four times the power supplied by PeakPW.

Figs. 4a and b compare the impacts in ozone concentrations between both scenarios. Although PeakPW produces less emissions than population weighted scenarios (PW2010), it results in similar impacts for ozone concentrations. Simulations show that if total emissions remain unchanged, ozone concentrations are most affected when emissions are increased during the day, i.e., when ozone production is significantly higher. Also, Fig. 4b exhibits a noticeable decrease in ozone in the basin's central area. Although PeakPW 2 NO<sub>x</sub> emissions are 20% lower than those of other scenarios (PermI-CEPW20), the impacts on ozone concentrations are higher. Impacts on ozone concentration, both increases and decreases, are more pronounced in scenario PeakPW 2 and ozone concentrations increase up to 4ppb over downwind locations in the eastern portion of the basin. If the same emissions are introduced, scenarios that concentrate them based on afternoon duty cycles have the potential to increase ozone concentrations more than cases in which emissions are introduced constantly during 24 hours.

#### 4.2.2. DG penetration

Socio-economic factors might lead to different adoption rates for DG technologies. For instance, DG technologies have the potential to meet 20% of the increased power demand by 2020 (CEC, 1999). Scenario EHP assumes the same DG technology mix as PW2010, but that 20% of the total energy demand will be supplied by DG. This fraction is 5.5 times higher than the market penetration of PW2010.

Fig. 4c shows the difference in ozone concentrations at 13:00 between EHP and the baseline. Results show that ozone consistently decreases in the basin's central areas. Also, there is a considerable ozone increase at downwind locations. Even though scenario EHP introduces the highest  $NO_x$  emission rates, the maximum increase in ozone concentration is less than 6 ppb. Also, ozone reductions are more pronounced in scenario EHP than PW2010 as the emissions introduced are higher. Impacts on ozone concentrations are smaller in EHP compared to those of PeakPW\_2. This confirms the importance of introducing emissions in duty cycles since EHP  $NO_x$  and VOC emissions are more than twice the emissions in PeakPW 2.

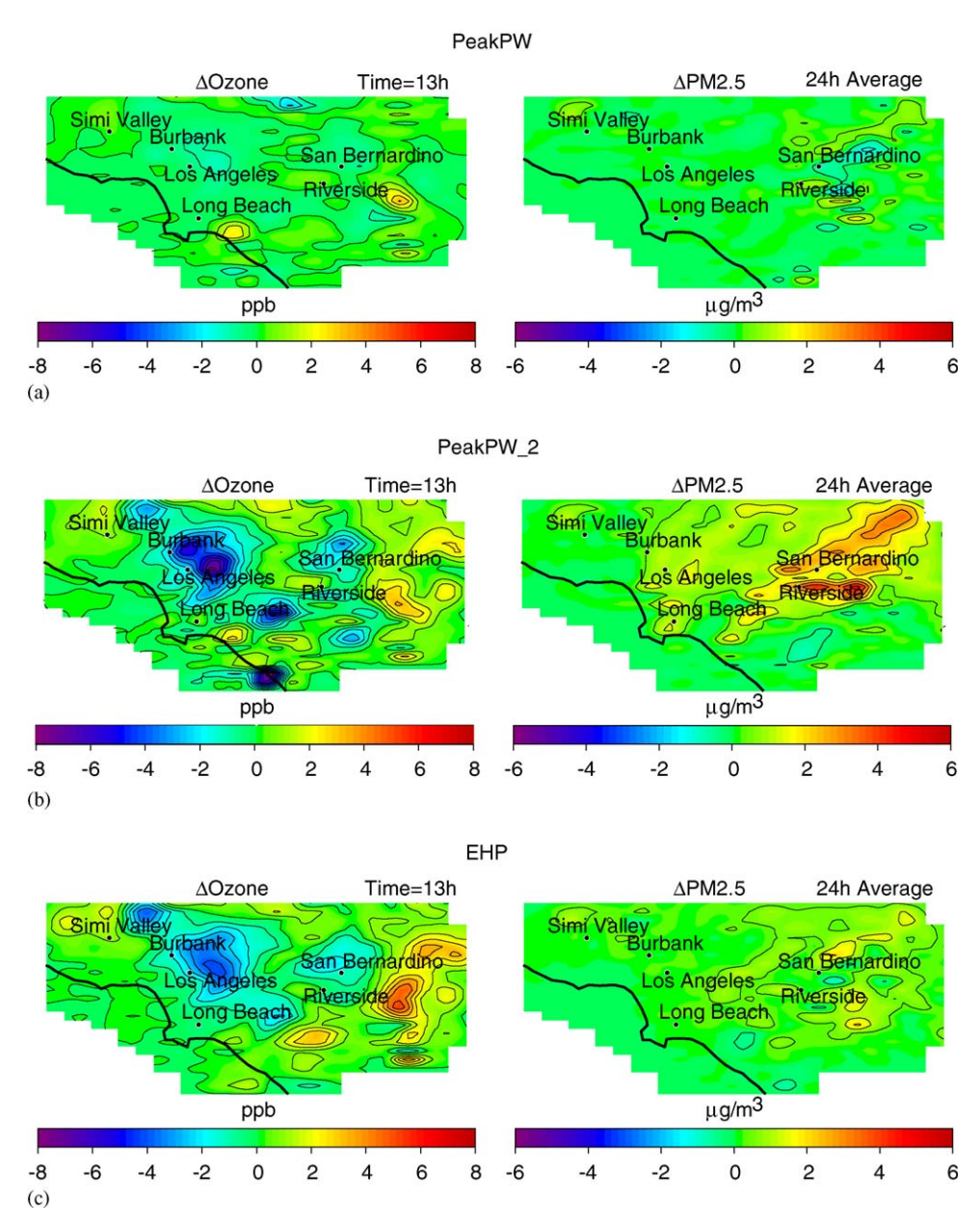


Fig. 4. Concentrations difference between DG scenarios and baseline for ozone and PM<sub>2.5</sub> aerosol. (a) PeakPW\_2, and (c) EHP. Ozone difference shown at hour 13:00. PM<sub>2.5</sub> difference shown for 24-h average concentrations.

Differences in 24-h average PM<sub>2.5</sub> concentration between the baseline and scenario EHP are presented in Fig. 4c. Scenario PeakPW\_2 produces larger impacts on PM<sub>2.5</sub> than EHP. Furthermore, from all spanning scenarios PeakPW\_2 leads to the highest increase in 24-h average PM<sub>2.5</sub> concentration. In both, EHP and PeakPW\_2, there is a net increase in PM<sub>2.5</sub> over the eastern side of the basin. In this region, nitric acid transported from Los Angeles combines with ammonia emitted

locally from cattle to form secondary particulate matter.

#### 5. Conclusions

This study investigates the effects on air quality due to the installation of DG units in the SoCAB by the year 2010. DG adoption scenarios have been developed with a general and systematic process, which includes the use of detailed data from GIS databases.

The scenarios are simulated in a state-of-the-art air quality model to assess environmental impacts of potential DG emissions throughout the SoCAB.

The most significant observable changes in ground level ambient ozone concentrations with respect to the baseline that result from DG emissions are approximately 7% for all realistic scenarios. Maximum  $PM_{2.5}$  relative changes up to 8% are observed for the realistic DG implementation scenario simulations. Modeling results for the realistic scenarios show that peak ozone and 24-h average  $PM_{2.5}$  concentrations do no exhibit any differences with respect to the baseline. However, maximum ozone changes due to DG range from 5 to -9 ppb. Maximum changes in 24-h average  $PM_{2.5}$  concentrations vary  $\pm 3 \,\mu \mathrm{g} \,\mathrm{m}^{-3}$  for realistic cases.

Three important caveats are: (1) the present study is based on simulations that use the 2010 nonattainment emissions inventory as the baseline, (2) most scenarios introduce only small ( $\sim 0.5\%$ ) total mass increments with respect to the projected baseline emissions, and (3) these maximum observable changes in ozone and PM<sub>2.5</sub> occur at specific locations and times in the simulation that may or may not affect compliance with air quality standards. Thus, DG air quality impacts may be significantly higher if the attainment scenario is used as the baseline or if a larger increment in the total mass emissions is introduced by DG. In addition, careful attention to the location and time of observed DG air quality impacts must be included before making a general conclusion regarding whether the air quality impacts are significant or of concern. Even when the air quality impacts estimated in this study are small, however, DG implementation may increase localized exposure to pollutants. Furthermore, higher levels of DG penetration in out years may also lead to significant impacts. For instance, DG installations may affect basin-wide compliance with air quality standards if their adoption occurs at higher levels or if their emission profiles result in higher emissions than those considered here.

This leads to the observable impacts of DG implementation for the spanning scenarios, which are more significant than those of the realistic scenarios. Maximum ground-level ozone increases are observed between 9% and 80% and maximum changes in PM<sub>2.5</sub> are observed up to 9% for the spanning scenario simulations. Spanning scenarios show that domain-wide ozone peak concentrations, compared to the baseline, increase only slightly for

the 2003ES, HEAPW20, BAU par, PeakPW 2 and EHP scenarios (1 ppb). In contrast, maximum 24-h average PM<sub>2.5</sub> vary  $\pm 2 \mu g \, m^{-3}$ . For ozone, the maximum hourly differences with respect to the baseline range from -26 to 34 ppb, whereas maximum changes in 24-h average PM<sub>2.5</sub> range from -4 to  $6 \mu g m^{-3}$ . Although spanning scenarios explore a variety of DG spatial distributions, the impact of DG spatial location on observed air quality impacts was small for the amount of DG emissions introduced in the current study. Also, several time-dependent DG implementation scenarios are examined. Results show that when DG emissions are produced during a 6-h period (peak duty cycle), they lead to a larger impact on air quality than the same amount of emissions introduced during a 24-h period (base load duty cycle).

# Acknowledgments

We graciously acknowledge the financial support of the California Energy Commission, sponsor of this work, and the significant leadership and contributions of Marla Mueller, our Contract Manager. M. Carreras and M. Medrano thank the continuing support of the Balsells-Generalitat de Catalunya Fellowship. M. Rodriguez acknowledges the support of the UC MEXUS Fellowship.

#### References

Allison, J.E., Lents, J., 2002. Encouraging distributed generation of power that improves air quality: can we have our cake and eat it too? Energy Policy 30 (9), 737–752.

CEC., 1999. Market assessment of CHP in the state of California.

Onsite Sycom Energy Corporation, prepared for California Energy Commission.

Gellins, C.W., Yeager, K.E., 2004. Transforming the electric infrastructure. Physics Today 57 (12), 45–51.

Griffin, R.J., Dabdub, D., Seinfeld, J.H., 2002a. Secondary organic aerosol 1. Atmospheric chemical mechanism for production of molecular constituents. Journal of Geophysical Research 107 (D17), 4332.

Griffin, R.J., Dabdub, D., Kleeman, M.J., Fraser, M.P., Cass, G.R., Seinfeld, J.H., 2002b. Secondary organic aerosol 3. Urban/regional scale model of size- and composition-resolved aerosols. Journal of Geophysical Research 107 (D17), 4334.

Griffin, R.J., Revelle, M.K., Dabdub, D., 2004. Modeling the oxidative capacity of the atmosphere of the South Coast Air Basin of California. 1. Ozone Formation Metrics. Environmental Science and Technology 38, 746–752.

Heath, A.G., Hoats, A.S., Nazaroff, W.W., 2003. Air pollutant exposure associated with distributed electricity generation. Prepared for the California Air Resources Board and the California Environmental Protection Agency. Contract #01-341.

- Ianucci, J., Horgan, S., Eyer, J., Cibulka, L., 2000. Air pollution emissions impacts associated with the economic market potential of distributed generation in California. Distributed Utility Associates, prepared for The California Air Resources Board. Contract #97-326.
- Marnay, C., Chard, J.S., Hamachi, K.S., Lipman, T., Moezzi, M.M., Ouaglal, B., Siddiqui, A.S., 2001. Modeling of customer adoption of distributed energy resources. Consortium for Electric Reliability Technology Solutions. Ernest Orlando Lawrence Berkeley National Laboratory, prepared for California Energy Commission.
- Medrano, M., Brouwer, J., Samuelsen, G.S., Carreras, M., Dabdub, D., 2003. Urban air quality impact of distributed generation, in ASME Turbo Expo 2003, Power for Land, Sea, and Air, Atlanta, Georgia, USA.
- Meng, Z., Dabdub, D., Seinfeld, J.H., 1998. Size-resolved and chemically resolved model of atmospheric aerosol dynamics. Journal of Geophysical Research 103 (D3), 3419–3435.
- Nguyen, K., Dabdub, D., 2002b. NO<sub>x</sub> and VOC control and its effects on the formation of aerosols. Aerosol Science and Technology 36, 560–572.

- Phi, V.M., Mauzey, J.L., McDonell, V.G., Samuelsen, G.S.,
   2004. Fuel injection and emissions characteristics of a commercial microturbine generator. Paper GT-2004-54039.
   ASME Turbo Expo: Power for Land, Sea and Air. Vienna,
   Austria, 14–17 June.
- Pun, B.K., Griffin, R.J., Seigneur, C., Seinfeld, J.H., 2002. Secondary organic aerosol 2. Thermodynamic model for gas/ particle partitioning of molecular constituents. Journal of Geophysical Research 107 (D17), 4333.
- Samuelsen, G.S., Brouwer, J., Medrano, M., 2003. Air quality impacts of distributed generation, final DG scenario development report. Prepared for the California Energy Commission, 500-00-033.
- Samuelsen, G.S., Brouwer, J., Medrano, M., Carreras, M., Dabdub, D., 2004. Air Quality Impacts of Distributed Generation, Final Report. Prepared for the California Energy Commission, Contract number 500-00-033.
- SCE., 2002. Southern California Edison Load Profiles. http://www.sce.com/sc3/005 regul info/005h sce profiles/default.htm.
- Tomashefsky, S., Marks, M., 2002. Distributed generation strategic plan. California Energy Commission.